RESEARCH ARTICLE

Microfluidic-Based ^{18}F-Labeling of Biomolecules for Immuno–Positron Emission Tomography

Kan Liu, Eric J. Lepin*, Ming-Wei Wang, Feng Guo, Wei-Yu Lin, Yi-Chun Chen, Shannon J. Sirk, Sebastian Olma, Michael E. Phelps, Xing-Zhong Zhao, Hsian-Rong Tseng, R. Michael van Dam, Anna M. Wu, and Clifton K.-F. Shen*

Abstract

Methods for tagging biomolecules with fluorine 18 as immuno–positron emission tomography (immunoPET) tracers require tedious optimization of radiolabeling conditions and can consume large amounts of scarce biomolecules. We describe an improved method using a digital microfluidic droplet generation (DMDG) chip, which provides computer-controlled metering and mixing of ^{18}F tag, biomolecule, and buffer in defined ratios, allowing rapid scouting of reaction conditions in nanoliter volumes. The identified optimized conditions were then translated to bench-scale ^{18}F labeling of a cancer-specific engineered antibody fragments, enabling microPET imaging of tumors in xenografted mice at 0.5 to 4 hours postinjection.

POSITRON EMISSION TOMOGRAPHY (PET) is a molecular imaging technique for biomedical research, drug development, and several clinical applications, including disease diagnosis and stage and assessment of therapeutic efficacy.[1,2] In combination with specific radiotracers, PET provides noninvasive whole-body visualization and quantification of normal biochemical processes as well as the onset, extent, and kinetics of pathologic processes in diseases.[3] ImmunoPET capitalizes on the selectivity of antibodies and their fragments and is emerging as an important approach for cancer imaging.[1] Recent advances in protein engineering have led to the generation of small antibody fragments and other protein binding scaffolds with high specificity and affinity to their targets; in vivo, these show good tumor targeting and accelerated blood clearance necessary for imaging. In clinical applications, fluorine 18 (^{18}F) offers the advantages of a short half-life (109.7 minutes), high positron yield (96.7%), and broad availability from existing radiopharmacy networks. With reduced molecular weights below the threshold for first-pass renal clearance, these proteins, when labeled with short-lived positron emitters such as ^{18}F, allow high-contrast, same-day imaging (1–6 hours postinjection). Therefore, the combination of a rapid-targeting protein format with easily accessible ^{18}F has strong potential for clinical development.

Current methods for direct ^{18}F labeling of small molecules using no-carried-added [^{18}F]fluoride often require anhydrous, strongly basic conditions at high temperature, which are not compatible with fragile biomolecules, such as proteins. Instead, the incorporation of [^{18}F]fluoride into proteins is usually achieved by using ^{18}F-labeled prosthetic groups, for example, *N*-succinimidyl 4-[^{18}F]fluorobenzoate ([^{18}F]SFB).[4] This is the most widely used ^{18}F-acylation reagent owing to its in vivo stability and radiochemical yield.[5] However, recent studies on ^{18}F labeling of antibody fragments using [^{18}F]SFB reported a low radiolabeling yield (RLY), which has prevented their more widespread adoption for preclinical studies and clinical translation.[6]

It is well established that biomolecule conjugation reactions employing acylation with Bolton-Hunter type reagents, such as *N*-succinimidyl esters, are strongly influenced by the solution pH and concentrations of the

*Authors who contributed equally to this work.

From the College of Electronics and Information Engineering, Wuhan Textile University, Wuhan, China; Department of Molecular and Medical Pharmacology, David Geffen School of Medicine at University of California, Los Angeles, Los Angeles, CA; Crump Institute for Molecular Imaging, Los Angeles, CA; California Nanosystems Institute, Los Angeles, CA; PET Center and Department of Nuclear Medicine, Cancer Hospital, Fudan University, Shanghai, China; and Department of Physics, School of Physics, and Center of Nanoscience and Nanotechnology, Wuhan University, Wuhan, China.

Address reprint requests to: Clifton K.-F. Shen, PhD, Crump Institute for Molecular Imaging, California NanoSystems Institute, UCLA, 570 Westwood Plaza, Los Angeles, CA, 90095; e-mail: kshen@mednet.ucla.edu.

DOI 10.2310/7290.2010.00043

DECKER

two reactants.[7–9] To obtain sufficient dose for microPET studies in an efficient and reproducible matter, performing small-scale experiments to explore several key reaction parameters to improve RLY, as well as specific activity (SA) and immunoreactivity, is necessary.[10] At bench scale, these efforts require large amounts of recombinant protein (on the order of milligrams) and repeated production of [^{18}F]SFB, discouraging the routine practice of such optimization procedures. In addition, the bench-scale approaches (even in the microliter scale) generally require manual operations, which are labor intensive and increase the risks of radiation exposure and operator error. An ideal solution would be to create a miniaturized reaction platform for screening a range of reaction conditions to identify optimal labeling parameters, with minimal consumption of biomolecules and radiolabeling agents.

Microfluidic devices, particularly based on the concept of using nanoliter droplets as microreactors, exhibit numerous advantages, including sample economy, precise control of reaction conditions, mixing, reproducibility, and scalability for various chemical and biologic applications.[11–17] Common methods of forming nanoliter droplets are creating emulsion by merging two immiscible fluids, such as water and oil. However, these implementations lack a practical means to generate composition-specific droplets on demand from scarce reagents, and most of them use oil as carriers, which might interfere with downstream chemical and biologic experiments.[12,17–21] Additional processes of oil removal and sample separation in a small volume can lead to significant loss of final product and elongate the total reaction time. Hence, reaction optimization using droplets (in oil) is often difficult to carry out in a reagent-economical fashion, a significant challenge when only small amounts of specialized biomolecules are available for labeling. On the other hand, using integrated microvalves, microfluidic batch reactors have demonstrated the digital automation and execution of complex on-chip chemical reactions and processes.[15,22–24] Therefore, a promising approach would be to confer digital control on an oil-free droplet generator by incorporating integrated microvalves into microchannel networks,[25] thus enabling sophisticated nanoliter-sized batch reactions and assays, which can be effectively harnessed for optimization of radiolabeling.

Herein we demonstrate a new method for performing rapid screening and optimization of reaction parameters (pH and concentration) for labeling an anti–prostate stem cell antigen (PSCA) diabody (A2 Db) with [^{18}F]SFB. The entire process was carried out in a very sample-economical fashion by using a novel microvalve-based digital microfluidic droplet generation (DMDG) chip in an oil-free environment. The production of ^{18}F-labeled A2 Db (4-[^{18}F]fluorobenzolyated A2 Db, ie, [^{18}F]FB-A2 Db) was successfully scaled up to produce sufficient quality and quantities of tracer for imaging mice with human prostate cancer xenografts.

Materials and Methods

Materials

Unless otherwise specified, all chemicals were of analytic grade and were commercially available. The preparations of ^{18}F-labeling agent, [^{18}F]SFB, and A2 Db are illustrated in the Supplementary Material. The prostate cancer xenograft LAPC-9, the B-cell lymphoma SKW6.4, and the PSCA-transduced SKW 6.4 cell lines were maintained as previously described.[26,27]

Chip Structure and Operation

The microfluidic chip system was designed to provide a reliable miniaturized platform to generate composition-controlled droplets for screening labeling parameters using very small amounts of reagents. A two-layer microvalve-based DMDG chip was designed composed of three functional parts: (1) a droplet generation core, where specific quantities of reagents are measured and merged into composition-specific droplets; (2) a peristaltic pump, which produces serial compressed nitrogen pulses that can precisely deliver intact droplets to the desired location at constant speed; and (3) a mixing channel for facilitating mixing process within each droplet (Figure 1, A and B). Inlets (from left to right) of droplet generation core are for cleaning solution 1, vacuum, cleaning solution 2 or buffer solution 1, [^{18}F]SFB, A2 Db, buffer solution, and pH control buffer 2, respectively, and port 8 is the outlet for waste.

In a typical experiment, [^{18}F]SFB and A2 Db solutions are pipetted into small transfer vials (from 5 to 20 μL), which served as reservoirs to continuously supply reactants during optimizing the radiolabeling reactions. By actuating the microvalves using control channels with compressed air (≈414 kPa), a series of on-chip functions and operations can be executed. The droplets (≈120 nL/droplet) composed of three ratio-controlled components are produced one by one (Figure 1C). The droplet generation process is digitally controlled by a computer within the droplet generation core and the sequences are as follows (see Supplementary Material for details): (1) vacuum is applied to remove residual gas inside each chamber; (2) the chamber is then filled with a different reagent (section I, II, and III in Figure 1B); (3) the

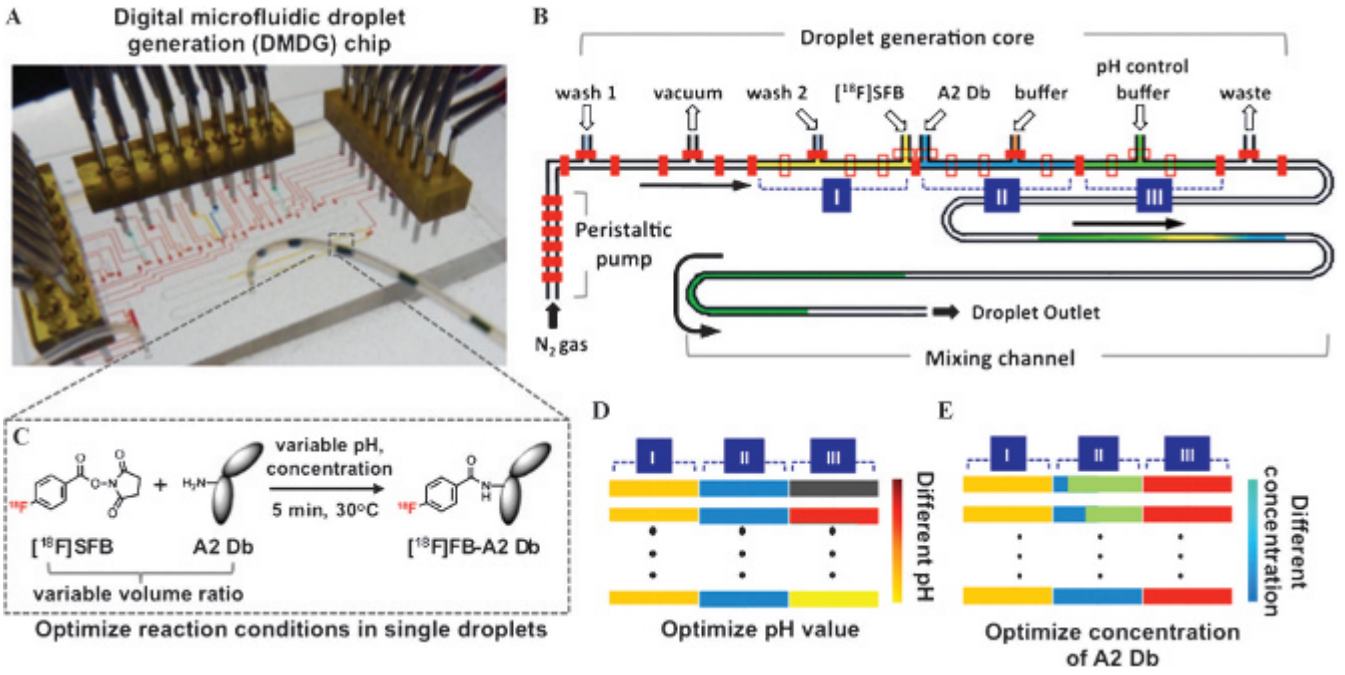

Figure 1. Schematic illustrations of the detailed architecture of a digital microfluidic droplet generation (DMDG) chip, working principle, and chip-based screening. *A*, A setup of a DMDG chip in which food dyes were used to aid visualization of different components. *B*, Schematic of a DMDG chip. The DMDG chip is composed of three functional parts: (1) a droplet generation core, where droplets with specific compositions can be generated digitally; (2) an on-chip peristaltic pump, which precisely produces serial compressed nitrogen pulses that can reliably deliver intact droplets to the desired location; and (3) a mixing channel. Inlets 1 to 8 are for cleaning, vacuum, cleaning/buffer 1, [^{18}F]SFB, A2 Db, buffer 2, pH control buffer, and waste, respectively. Section I is specifically used for [^{18}F]SFB, section II for A2 Db and buffer 2, and section III for pH control buffer, respectively. The fluidic channel width is approximately 200 μm and the height is approximately 40 μm. *C*, The reaction scheme of ^{18}F-labeling diabody using [^{18}F]SFB. *D*, Schematic of adjusting pH in each droplet. *E*, Schematic of adjusting the concentration of A2 Db in each droplet.

dividing microvalves are opened and their contents are merged to form a single multicomponent droplet; and (4) the droplets with specific compositions are driven into the mixing channel by compressed nitrogen. By changing reagents and/or adjusting the chamber volumes, droplets with predetermined compositions can be generated. In general, it takes approximately 1 minute to generate five droplets representing a given ^{18}F-labeling reaction condition. On-chip digital control to manipulate small volumes has enabled sophisticated nanoliter-sized batch reactions. In addition, the oil-free droplets can be directly collected, measured, and used for the next step.

Adjustment of pH Condition

To adjust the pH value of each ^{18}F-labeling reaction, different pH control buffers with a fixed volume (five-chamber units [≈40 nL], section III in Figure 1D) were introduced into each droplet along with the [^{18}F]SFB and A2 Db (v/v/v, 1:1:1) (see Supplementary Material, Figure S6 and Table S3 for details). After cleaning the droplet generation core and mixing channel, the pH value in each droplet can be easily adjusted by using a desired pH control buffer. Eleven standard pH control buffers (pH 4.0, 4.5, 5.0, 5.5, 6.0, 8.0, 8.7, 10.0, 11.0, 12.0, 13.0) were applied for adjusting the pH range in each ^{18}F-labeling reaction condition.

Adjustment of A2 Db Concentration

To adjust the concentration of A2 Db, section II in the droplet generator core was subdivided by microvalves into two individual chambers with different size ratios, which were then filled with A2 Db solution and dilution buffer (Figure 1E), respectively. Using an A2 Db stock solution (2 mg/mL in optimized pH buffer), droplets with seven different concentrations (from 0.13 to 1.3 mg/mL) were generated on-chip by combining sections II and III (see Supplementary Material).

Sample Collection and Radiochemistry Analysis

Sample droplets were stored and reacted within the sample outlet tube for 5 minutes and then directly dropped onto

instant thin layer chromatography (iTLC) strips (Biodex, Shirley, NY) for analysis. The final RLYs were determined by a gamma counter (Wizard 3, Perkin Elmer, Waltham, MA). To avoid cross-contamination between droplets of different pH, wash droplets (a combination of deionized water/pH 7.4 phosphate-buffered saline [PBS] buffer) were inserted between droplets for cleaning (see Supplementary Material, Table S2).

Estimation of Effective Specific Activity

Because the separation of [^{18}F]FB-A2 Db from A2 Db is practically difficult, the ratio of radioactivity of ^{18}F-labeled diabody over total mass of diabody used in radiolabeling reaction ([^{18}F]FB-A2 Db/A2 Db) is used to define effective specific activity (ESA). To determine the radioactivity of [^{18}F]FB-A2 Db, radioactivity was measured by a dose calibrator (CRC-25R, Capintec, Ramsey, NJ). The concentration of A2 Db stock solutions was determined by ultraviolet (UV) absorption (at 280 nm). The molecular weight of A2 Db and its extinction coefficient were calculated based on its amino acid sequence (ProtParam Tool, ExPASy, SIB). Calculated ESAs were derived by dividing the radioactivity of [^{18}F]FB-A2 Db from the reaction mixture by the total amount of diabody (in mmol, based on a molecular weight of 55,000 Da). The radioactivity of [^{18}F]FB-A2 Db was corrected by the radiochemical purity of crude reaction mixture determined by iTLC analysis.

Scale-up Using Optimized Condition

A larger amount of [^{18}F]FB-A2 Db was produced at bench scale under the optimized condition. RLYs were measured by iTLC and size-exclusion high-performance liquid chromatography (SEC-HPLC) (Biosep SEC S-2000, Phenomenex, Torrance, CA). Radiolabeled diabody was purified by a spin column (Micro Biospin 6 column, Bio-Rad, Hercules, CA). The radiochemical purity of [^{18}F]FB-A2 Db was determined by iTLC and SEC-HPLC (PBS buffer [pH 7.4], flow rate 1 mL/min, UV wavelengths 254 and 280 nm, retention time [t_R]= 5.1 min).

Immunoreactivity Assay

The immunoreactive fraction of [^{18}F]FB-A2 Db was determined by incubating its SEC-HPLC purified fraction (0.1 μCi [≈0.01 μg]) with large excess (≈2×10^7 cells) of either SKW6.4-PSCA (PSCA overexpressing) cells, SKW6.4 cells (negative control), or no cells in 1 mL (PBS, 1% fetal bovine serum) for 40 minutes at room temperature. After incubation, cells were spun down (800*g*) and 0.7 mL of supernatant was counted in a gamma counter. Experiments were carried out in duplicate. The immunoreactivity was determined as the fraction that bound to the cells (SKW6.4-PSCA) compared to the control (no cells).

MicroPET/CT Imaging and Biodistribution Studies

All animal studies were conducted under protocols approved by the Chancellor's Animal Research Committee at the University of California, Los Angeles. LAPC-9 xenografts were established in 7- to 8-week-old male SCID mice (Charles River Laboratories, Wilmington, MA) by subcutaneous inoculation of LAPC-9 cells (≈10^6 cells) near the shoulder. After 14 to 21 days, when tumor masses were in the range of 100 to 300 mg, [^{18}F]FB-A2 Db (50–99 μCi) was injected into the tail vein of each animal. Mice were serially imaged using a microPET scanner (Focus 220, Siemens Preclinical Solutions, Knoxville, TN). To enable imaging, mice were anesthetized using 2% isoflurane, positioned in a prone position along the long axis of the microPET scanner, and imaged. Images were reconstructed using a filtered backprojection reconstruction algorithm. Directly after the microPET scan, a computed tomographic (CT) scan was performed using a microCT scanner (microCAT II, Concorde Microsystems, Knoxville, TN) for 10 minutes. After the final CT scan, mice were euthanized and tumors, liver, spleen, kidney, lung, and blood were harvested, weighed, and counted in a gamma counter. The results were calculated as the percentage of injected dose per gram of tissue. For image analysis, cylindrical regions of interest (ROI) were drawn from three-dimensional filtered backprojection reconstructed PET/CT coregistered images using AMIDE as previously described. Four ROI were drawn within the tumor and another four in the arm muscle region in the low-activity areas close to the tumors and termed ''background.''

Results

Optimization of pH and Concentration on Chip

Using our DMDG chip, we rapidly screened 11 radiolabeling conditions with different pHs, ranging from 5 to 10. At a constant A2 Db concentration (stock solution 2 mg/mL; droplet 0.66 mg/mL in PBS buffer [pH 7.4]), the maximum RLY was obtained at pH 8.7 (see Supplementary Material, Figure S7). To confirm these findings, the pH of A2 Db stock solution was readjusted to 8.7, the screening

experiments were repeated, and the results again showed that the optimal pH was indeed 8.7 (n = 5; Figure 2A). Separately, we also confirmed that A2 Db was stable over a pH range of 7.5 to 10 and showed very little loss in binding activity (see Supplementary Material, Figure S2b). Using our DMDG chip, the concentration of A2 Db in each droplet (ranged from 0.13 to 1.33 mg/mL) was generated by changing the volume ratios between A2 Db and pH 8.7 buffer in sections II and III in the droplet generation core (see Supplementary Material, Figure S8). As shown in Figure 2B, the RLY of diabody with [^{18}F]SFB was strongly concentration dependent. The RLY was ≈8% at the A2 Db concentration of 0.25 mg/mL and increased to 27% at 1 mg/mL.

Determination of Optimal Conditions

The calculated ESAs were determined based on the final radioactivity of [^{18}F]FB-A2 Db according to RLYs in each microfluidic-based experiment and the amount of Db in each droplet. Although RLYs of diabody labeling reactions increased as the concentration of Db increased (see Figure 2B), the ESAs actually declined at Db concentrations above 0.5 mg/mL. Therefore, to maintain a reasonably high labeling yield to provide a sufficient amount of [^{18}F]FB-A2 Db for microPET studies while obtaining tracers with the highest SA, we selected 0.66 mg/mL (pH 8.7) as the optimal concentration for scale-up.

Scale-up from Microfluidics to Bench Scale

Prior to scale-up, it is critical to determine whether the optimal labeling conditions obtained on-chip could be directly translated into a bench-scale run. To do so, we repeated the pH optimization study off-chip using a bench-scale reaction. [^{18}F]SFB (25 μL in PBS buffer [pH 7.4]) and A2 Db (50 μL [1 mg/mL] in buffers with various pHs) were mixed and incubated in vials at 30°C for 5 minutes. In these bench-scale experiments, maximal RLY (25.8%) was also observed at pH 8.7 (Figure 2D), demonstrating good agreement between optimal conditions found by bench-scale and on-chip approaches. Small batches of [^{18}F]FB-A2 Db from on-chip and bench-scale labeling were produced under the optimized labeling conditions (A2 Db concentration 0.66 mg/mL in sodium borate buffer [pH 8.7] for 5 minutes at 30°C). Size-exclusion chromatographic analyses (SEC-HPLC) of those two crude reaction mixtures showed high similarity (see Supplementary Material, Figure S9). Following a simple spin-column purification, sodium dodecyl sulfate–polyacrylamide gel electrophoresis (SDS-PAGE) and autoradiographic imaging (Figure 2C) analyses also confirmed the formation of [^{18}F]FB-A2 Db with high radiochemical purity in both approaches. The radiochemical purity of [^{18}F]FB-A2 Db was also determined by SEC-HPLC (> 95%) (see Supplementary Material, Figure S10). Under the optimized condition, about 6 to 10 mCi of [^{18}F]FB-A2 Db was produced from 20 to 35 mCi of [^{18}F]SFB in 10 to 20 minutes.

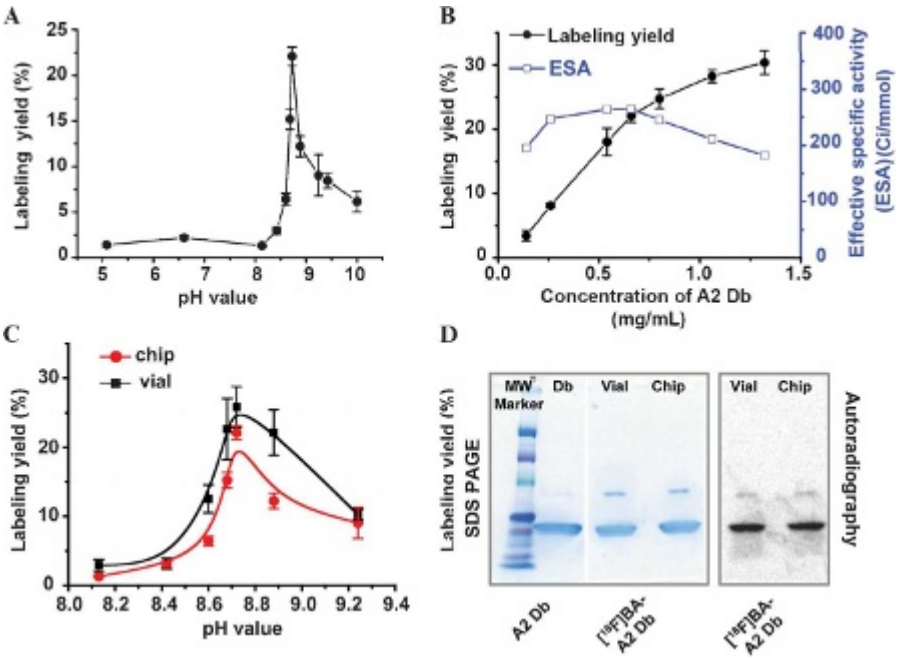

Figure 2. *A*, The effect of pH on RLY (n = 3). *B*, The effect of diabody concentration on RLY at pH 8.7 (n = 3). *C*, Unlabeled A2 Db and [^{18}F]FB-A2 Db produced from bench-scale vial and microfluidic chip were run on SDS-PAGE and analyzed by autoradiography. Proteins were later revealed by Coomasie blue staining. *D*, Compare RLY by using the conventional bench-scale method and on-chip approach (n = 3).

Immunoreactivity

It is of critical importance that proteins, such as diabodies, still retain their biologic function after ^{18}F-labeling. Using PSCA-overexpressing SKW 6.4-PSCA cells and parental SKW 6.4 cells (negative control), the immunoreactivity of purified [^{18}F]FB-A2 Dbs prepared from both approaches (microfluidic and bench scale) was determined. After 40 minutes' incubation with cells at ambient temperature, both [^{18}F]FB-A2 Dbs showed similar high immunoreactivities (≈68 ± 1% [SD], Figure 3A).

MicroPET/CT Imaging and Biodistribution Studies

The calculated ESAs of the final [^{18}F]FB-A2 Dbs ranged from 14.8 to 20.4 TBq/mmol (400–550 Ci/mmol) after a simple spin-column purification, and radiochemical purities were > 95% (see Supplementary Material, Figure S10). In a typical microPET study, [^{18}F]FB-A2 Db (85–100 μCi) was injected intravenously into tumor-bearing mice (n = 3), and a dynamic scan was performed from 0 to 110 minutes (Figure 3B). Tumor locations were visualized on microPET/CT images ≈20 to 30 minutes postinjection owing to a combination of increased tumor signal and rapid blood clearance. As expected, the majority of the [^{18}F]FB-A2 Db cleared through the kidneys; a portion of the radioactivity cleared via the gallbladder and intestines, which was also observed for hydrolyzed [^{18}F]SFB (ie, 4-[^{18}F]fluorobenzoic acid) (see Supplementary Material, Figure S11). At 4 hours postinjection, microPET images showed that high tumor contrast and clear imaging were obtained (see Figure 3C) with a target to background ratio of 13.6 ± 2.5 determined by ROI analysis of LAPC-9 tumor versus soft tissue. This is consistent with the biodistribution data (4 hours postinjection), which demonstrated that most of the activity had cleared from major organs, resulting in a higher tumor uptake (3.13% injected dose per gram) compared to liver, spleen, kidneys, and lung uptake (Figure 3D). The tumor to blood ratio for the LAPC-9 tumors using [^{18}F]FB-A2 Db was 4.8 at 4 hours.

Discussion

Imaging of cell surface biomarkers is emerging as an increasingly important approach in cancer detection and monitoring therapeutic efficacy. We have previously shown that engineered antibody fragments (ie, diabodies and minibodies) retain excellent tumor targeting in mouse models in vivo, coupled with rapid clearance from the circulation. Given that the pharmacokinetics of diabodies matches very well with the half-life of ^{18}F,[6] their ^{18}F-labeled versions represent a novel class of PET tracers with broad potential utility for imaging the cell surface phenotype in vivo. Therefore, there is a great need for developing efficient procedures to produce ^{18}F-labeled diabody-based tracers in high yield sufficient for routine PET imaging.

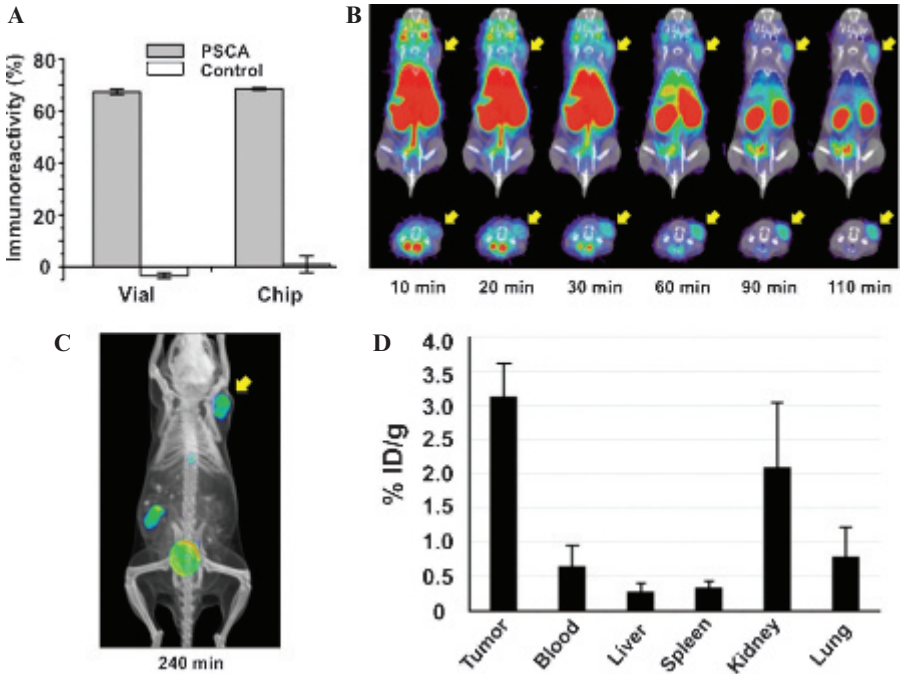

Figure 3. Biochemical in vitro and in vivo characterizations of [^{18}F]FB-A2 Db. *A*, Immunoreactivity of [^{18}F]FB-A2 Db produced from vial or chip to PSCA-expressing SKW 6.4 and SKW 6.4 cells (control) (n = 2). *B*, Coregistered microPET/CT dynamic scan images (coronal [*top*] and transverse [*bottom*] slices) of nude mice bearing LAPC-9 (PSCA-positive human prostate cancer) xenografts. Tumor locations are indicated by *yellow arrows*. *C*, A coregistered microPET/CT image (coronal projections) 4 hours postinjection of [^{18}F]FB-A2 Db. *D*, Graph of biodistribution study of [^{18}F]FB-A2 Db (4 hours postinjection) (n = 3).

Because the amounts of proteins produced in the research and development environment are often restrained, the extent to which trial-and-error optimizations of the [^{18}F]SFB labeling reactions can be conducted is rather limited. Alternatively, brute force approaches using entire batches of proteins and high activity (> 1 Ci) were often used to ensure sufficient activity produced for microPET studies.[6] Therefore, a practical means to perform optimization using only a small amount of proteins and radiolabeling tags is critical to the progress of this field. Given that the minute masses required for radiotracer production are well matched to the small volumes required in microfluidics, we have designed and fabricated a DMDG chip that can ''digitally'' generate composition-specific and size-controlled droplets on demand. This microfluidic-based optimization method provides a simple and effective means to perform screening pH and concentration droplet by droplet. The unique features of this device allow (1) the independent control of volume and composition for every droplet, enabling reaction condition screening with minimal reagent consumption (see Supplementary Material, Movie S1); (2) the ability to pause, modify, and restart the droplet generation process, for example, for replacement or change of reagents (see Supplementary Material, Movie S2); and (3) the use of nitrogen gas rather than oil to separate droplets, eliminating the need for oil removal steps later. Furthermore, the current device, distinct from other droplet-based microfluidics,[14,28] is unique in its ability to operate with very low total volumes of samples and reagents with little to no loss. As each droplet can be driven out slowly in a well-controlled matter using the on-chip peristaltic pump, one single droplet can be easily used for determining the corresponding RLY. The volume and radioactivity of a single droplet are around 120 nL and 0.5–2 μCi, respectively. For example, 5 μL of diabody solution (2 mg/mL) could be used in screening for more than 125 different conditions in single microdroplets.

To probe a specific biologic process in vivo without exerting mass effects within the same living systems under study, for example, measuring receptor–ligand interactions, PET tracers with high SA are desired. Our strategy to obtain ^{18}F-labeled diabody of high SA (in our case, ESA) is to, first, identify the pH range leading to the highest RLY and subsequently to optimize the protein concentration to generate the highest ESA at the previously determined optimal pH. In the [^{18}F]SFB labeling reactions, RLYs generally increase at higher protein concentrations at the optimal pH. However, continuing to increase the amount of protein used in the labeling reaction will lower the final ESA because the RLY eventually plateaus (see Figure 2B). Using our DMDG chip, a series of experiments with different pHs and concentrations can be rapidly performed, allowing mapping of the area of optimal conditions. This is especially important because the optimal parameters for [^{18}F]SFB labeling vary depending on the sequence and structure of the individual protein being radiolabeled. Furthermore, batch-to-batch variations can occur for the protein and [^{18}F]SFB as well, making rapid optimization using small aliquots of reactants even more critical. Our method using the DMDG chip can address requirements above by identification of optimal reaction parameters in a rapid, reagent-economical fashion. Once the optimal reaction parameters are identified, larger-scale reactions can be performed under the same chip-derived conditions to produce a sufficient amount of ^{18}F-labeled biomolecules.

Compared to the previously described ^{124}I-labeled minibody currently in clinical development,[29] the new [^{18}F]FB-A2 Db opens the possibility of same-day PET imaging with superior image contrast in a clinical setting. The key advantage of using diabodies, the smallest bivalent fragments based on antibody combining sites, is the potential to obtain clear tumor visualization just a few hours (4–6 hours) after injection.[30] Earlier microPET imaging results using ^{124}I-labeled anti-PSCA diabodies suggested that the best image contrast required a 12-hour delay and the tumor to blood (ROI) ratio was around 3.[31] In contrast, the tumor to soft tissue ratio using [^{18}F]FB-A2 Db in this study was 13.6 at 4 hours postinjection, which represents a significant improvement. There are several possible explanations for this improvement. First, the half-life and positron yield of ^{18}F is better suited for PET detection within 4 to 6 hours postinjection. Second, owing to the optimization of the microfluidic method, the resulting [^{18}F]FB-A2 Db was obtained with high immunoreactivity to PSCA, radiochemical purity, and ESA. Third, the radioiodination method used to label anti-PSCA diabodies[27] was not optimal and could result in deiodination that can affect the tumor uptake and reduce image contrast. It is difficult to isolate the degree of influence among those individual parameters from in vivo imaging results, and it is likely that all of the factors listed above are important. Regardless, to obtain an effective protein-based immunoPET tracer, it is necessary to optimize individual ^{18}F-labeling conditions under which a sufficient amount of tracer with high immunoreactivity, ESA, and radiochemical purity can be generated.

To show the versatility and generality of our method, we also applied this microfluidic-based method to optimize the [^{18}F]SFB labeling of an additional diabody (anti-HER2 Db) specific to human epidermal growth factor receptor 2 (HER2), and, under optimized conditions (see Supplementary Material, Figure S12), [^{18}F]FB-anti-HER2 Db was obtained for microPET studies in a breast cancer xenograft-bearing mouse (MCF-7/HER2) (see Supplementary Material, Figure S13). These successful examples using a microfluidic-based approach for optimization of labeling conditions provide a practical means to produce [^{18}F]fluorobenzoylated diabodies ([^{18}F]FB-labeled Dbs) or other scarce biomolecules. Furthermore, our microfluidic-based method is a de novo approach and can be applied in the beginning of each labeling experiment to access the quality of biomolecules and determine the best labeling condition for the day.

Conclusion

A rapid and efficient method was developed to ^{18}F-label diabodies by scouting conditions using a DMDG chip. Reaction parameters (pH and diabody concentration) were analyzed in individual droplets, requiring only very small amounts of protein (diabody) and [^{18}F]SFB. A 200- to 2,000-fold reduction in protein consumption can be achieved, compared to conventional bench-scale approaches, during the optimization stage. Optimal labeling conditions identified by a DMDG chip were then translated into efficient scale-up of [^{18}F]FB-A2 Db suitable for in vivo evaluation. This versatile microfluidic-based method has the potential to be employed efficiently for radiolabeling of a diverse spectrum of biomolecules, including intact antibodies and their fragments, other proteins, and peptides, which can ultimately accelerate investigations using novel biologic PET tracers.

Acknowledgments

We thank N. Satyamurthy and his staff for providing ^{18}F ion and many useful discussions; H.-D. Lin, C. Xia, and D.A. Williams for assisting with radiolabeling chip and system design; R. Reiter and colleagues for providing the mouse models; and T. Olafsen, D. Stout, W. Ladno, and J. Edwards for assistance with the microPET studies.

Financial disclosure of authors: This work was supported by funding from the US Department of Energy (DE-PS02-09ER09-08 and DE-PS02-09ER09-18), the National Institutes of Health (R21 EB008419-01, CA 092131 and CA 086306), a University of California Discovery Grant (bio07-10665), and the UCLA Jonsson Comprehensive Cancer Center (CA016042).

Financial disclosure of reviewers: None reported.

References

1. Phelps ME. Positron emission tomography provides molecular imaging of biological processes. Proc Natl Acad Sci U S A 2000;97:9226–33.
2. Czernin J, Phelps ME. Positron emission tomography scanning: current and future applications. Annu Rev Med 2002;53:89–112.
3. Weber WA. Positron emission tomography as an imaging biomarker. J Clin Oncol 2006;24:3282–92.
4. Vaidyanathan G, Zalutsky MR. Labeling proteins with F-18 using N-succinimidyl 4-[F-18]fluorobenzoate. Nucl Med Biol 1992;19:275–81.
5. Okarvi SM. Recent progress in fluorine-18 labelled peptide radiopharmaceuticals. Eur J Nucl Med 2001;28:929–38.
6. Cai WB, Olafsen T, Zhang XZ, et al. PET imaging of colorectal cancer in xenograft-bearing mice by use of an F-18-labeled T84.66 anti-carcinoembryonic antigen diabody. J Nucl Med 2007;48:304–10.
7. Li JL, Trent JO, Bates PJ, Ng CK. Factors affecting the labeling yield of F-18-labeled AS1411. J Labelled Compd Rad 2007;50:1255–9.
8. Zijlstra S, Gunawan J, Burchert W. Synthesis and evaluation of a F-18-labelled recombinant annexin-V derivative for identification and quantification of apoptotic cells with PET. Appl Radiat Isotopes 2003;58:201–7.
9. Garg PK, Garg S, Zalutsky MR. F-18 labeling of monoclonal-antibodies and fragments with preservation of immunoreactivity. Bioconjugate Chem 1991;2:44–9.
10. Vaidyanathan G, Zalutsky MR. Protein radiohalogenation: observations on the design of N-succinimidyl ester acylation agents. Bioconjug Chem 1990;1:269–73.
11. Talu E, Hettiarachchi K, Zhao S, et al. Tailoring the size distribution of ultrasound contrast agents: possible method for improving sensitivity in molecular imaging. Mol Imaging 2007;6:384–92.
12. Liu K, Ding HJ, Liu J, et al. Shape-controlled production of biodegradable calcium alginate gel microparticles using a novel microfluidic device. Langmuir 2006;22:9453–7.
13. Thorsen T, Maerkl SJ, Quake SR. Microfluidic large-scale integration. Science 2002;298:580–4.
14. Song H, Chen DL, Ismagilov RF. Reactions in droplets in microflulidic channels. Angew Chem Int Edit 2006;45:7336–56.
15. Lee CC, Sui GD, Elizarov A, et al. Multistep synthesis of a radiolabeled imaging probe using integrated microfluidics. Science 2005;310:1793–6.
16. Mark D, Haeberle S, Roth G, et al. Microfluidic lab-on-a-chip platforms: requirements, characteristics and applications. Chem Soc Rev 2010;39:1153–82.
17. Liu K, Ding HJ, Chen Y, Zhao XZ. Droplet-based synthetic method using microflow focusing and droplet fusion. Microfluid Nanofluid 2007;3:239–43.
18. Hong JW, Quake SR. Integrated nanoliter systems. Nat Biotechnol 2003;21:1179–83.
19. Pregibon DC, Toner M, Doyle PS. Multifunctional encoded particles for high-throughput biomolecule analysis. Science 2007;315:1393–6.

20. Beer NR, Hindson BJ, Wheeler EK, et al. On-chip, real-time, single-copy polymerase chain reaction in picoliter droplets. Anal Chem 2007;79:8471–5.
21. Abdelgawad M, Watson MWL, Wheeler AR. Hybrid microfluidics: a digital-to-channel interface for in-line sample processing and chemical separations. Lab Chip 2009;9:1046–51.
22. Wang JY, Sui GD, Mocharla VP, et al. Integrated microfluidics for parallel screening of an in situ click chemistry library. Angew Chem Int Edit 2006;45:5276–81.
23. Gerber D, Maerkl SJ, Quake SR. An in vitro microfluidic approach to generating protein-interaction networks. Nat Methods 2009;6:71–4.
24. Chung KH, Crane MM, Lu H. Automated on-chip rapid microscopy, phenotyping and sorting of C. elegans. Nat Methods 2008;5:637–43.
25. Liu K, Chen Y, Tseng H, et al. Microfluidic device for robust generation of two-component liquid-in-air slugs with individually controlled composition. Microfluid Nanofluid 2010. DOI:10.1007/s10404-010-0617-0.
26. Craft N, Chhor C, Tran C, et al. Evidence for clonal outgrowth of androgen-independent prostate cancer cells from androgen-dependent tumors through a two-step process. Cancer Res 1999;59:5030–6.
27. Leyton JV, Olafsen T, Lepin EJ, et al. Humanized radioiodinated minibody for imaging of prostate stem cell antigen-expressing tumors. Clin Cancer Res 2008;14:7488–96.
28. Teh SY, Lin R, Hung LH, Lee AP. Droplet microfluidics. Lab Chip 2008;8:198–220.
29. Gagnon P, Cheung CW, Lepin EJ, et al. Minibodies and multimodal chromatography methods. Bioprocess Int 2010;8:26–35.
30. Wu AM, Yazaki PJ. Designer genes: recombinant antibody fragments for biological imaging. Q J Nucl Med 2000;44:268–83.
31. Leyton JV, Olafsen T, Sherman MA, et al. Engineered humanized diabodies for microPET imaging of prostate stem cell antigen-expressing tumors. Protein Eng Des Sel 2009;22:209–16.